

VINE RESIDUE-DERIVED ENGINEERED BIOCHAR FOR ENVIRONMENTAL BENEFITS

Suzana Ioana CALCAN¹, Oana Cristina PÂRVULESCU^{2*}, Violeta Alexandra ION³, Cristian Eugen RĂDUCANU⁴, Tănase DOBRE⁵, Gabriel VASILIEVICI⁶, Andrei BURGHELEA⁷

Relevant aspects regarding the production and application of biochar (BC) and chemically activated biochar (ABC) are presented in the paper. Vine pruning residues, either non-impregnated or impregnated with phosphoric acid (H_3PO_4), were pyrolyzed under different operating conditions. Slow pyrolysis tests were conducted in a fixed bed column, in the presence of CO_2 as a sweeping gas, for 60 min, obtaining BC/ABC, bio-oil, and pyrolysis gases. Heat flux ($q = 4.3\text{--}6.6\text{ kW/m}^2$) and impregnation ratio ($IR = 0\text{--}2.2\text{ g/g}$) were selected as pyrolysis process factors. BC and ABC obtained in 12 pyrolysis experimental runs were tested as adsorbents of 1,2-dichloroethane (DCE) from air stream. Fixed bed adsorption experiments were performed at 40 °C for 90 min. Final values (at 60 min for pyrolysis and 90 min for adsorption) of specific mass of BC/ABC (0.310–0.542 g/g), specific mass of bio-oil (0.230–0.334 g/g), mean temperature of BC/ABC bed (345–422 °C), and BC/ABC adsorption capacity for DCE (0.064–0.136 g/g) were chosen as dependent variables. The effects of process factors on dependent variables were quantified using quadratic polynomial models that fitted the experimental data well. These regression models were used to determine the optimum levels of process factors, i.e., $q = 6.6\text{ kW/m}^2$ and $IR = 1.1\text{ g/g}$, for which maximum predicted values of adsorption capacity (0.137 g/g), specific mass of bio-oil (0.318 g/g), and mean temperature of BC/ABC bed (420 °C) were obtained.

Keywords: adsorption, engineered biochar, impregnation, pyrolysis, vine pruning residue

¹ Ph.D. Student, Dept. of Chemical and Biochemical Engineering, National University of Science and Technology POLITEHNICA Bucharest, Romania

² * Prof., Dept. of Chemical and Biochemical Engineering, National University of Science and Technology POLITEHNICA Bucharest, Romania, corresponding author, e-mail: oana.parvulescu@yahoo.com ()

³ PhD Eng., USAMV Bucharest, Romania

⁴ PhD Eng., Dept. of Chemical and Biochemical Engineering, National University of Science and Technology POLITEHNICA Bucharest, Romania

⁵ Prof., Dept. of Chemical and Biochemical Engineering, National University of Science and Technology POLITEHNICA Bucharest, Romania

⁶ Research Scientist I, ICECHIM Bucharest, Romania

⁷ Master Student, Dept. of Analytical Chemistry and Environmental Engineering, National University of Science and Technology POLITEHNICA Bucharest, Romania

1. Introduction

There is an obvious propensity lately towards the valorization of residues from the agro-industrial sector, one of the largest producers of residual materials [1–3]. The increasing amount of agro-industrial residues is a pressing global problem that needs to be solved by converting them into sustainable products. Biochar is a carbon-rich, renewable, cheap, and sustainable material that is obtained from various organic residues and can have significant agronomic, environmental, and economic benefits [3–7].

Biochar is usually produced by slow pyrolysis of organic materials, at heating rates of 0.1–1 °C/s, temperatures of 300–700 °C, and in the presence of a sweeping gas that can be inert (N₂, Ar) or oxidizing (CO₂, steam) [1,2,7–9]. Its yield and properties are mainly affected by the type and pretreatment of feedstock, type and superficial velocity of sweeping gas, heating rate, operating temperature and time [4,8,10,11]. Biochar properties, especially porosity, pore structure, specific surface area (SSA), water holding capacity (WHC), pH, mineral composition, surface charge, and surface functional groups (SFGs), determine its applications [4,7,12–14]. It is useful as a soil amendment, contaminant adsorbent, renewable fuel, activated carbon (AC) or AC precursor, supported catalyst (SC) or SC precursor [4,7,10–17].

Pristine BC is obtained from unmodified feedstock without sweeping gas or in the presence of an inert gas. Its efficiency can be improved by physical or chemical activation (*e.g.*, physical activation with CO₂ or steam, chemical modification with acids, bases, metal salts or oxides), resulting in engineered biochar with properties tailored for specific applications [4,10–14]. Engineered biochar is widely used for removing pollutants from water and air [2,4,7,10–14,18–20]. Compared to the removal of water pollutants, there are few studies in the related literature on its application for the retention of air pollutants, *e.g.*, acid gases (CO₂, SO₂, H₂S), nitrogen oxides (NO_x), volatile organic compounds (VOCs) [4,7,14,18–20]. Engineered biochar retains air pollutants mainly through adsorption [7,13]. Its adsorption capacity depends on different factors, including biochar properties (porosity, pore structure, SSA, SFGs), nature and initial concentration of pollutant species, process temperature [10,18–20].

The properties of the engineered biochar and therefore its adsorption capacity can be significantly affected by the activation process. Physical activation with oxidizing gases (CO₂ or steam) introduces oxygen-containing SFGs and leads to numerous pores in the material structure, especially micropores [7,12]. Oxygen-containing SFGs facilitate the sorption of inorganic and polar organic contaminants [4]. Chemical treatment with acids (HNO₃, HCl, H₂SO₄, H₃PO₄), bases (KOH, NaOH), metal salts (MgCl₂, ZnCl₂, AlCl₃, FeCl₃, K₂CO₃) or oxides (CaO, MgO, MnO, ZnO, TiO₂, Fe₂O₃), which is performed either before or after pyrolysis,

generally promotes the formation of micropores, increases SSA and SFGs, thereby improving the sorption capacity of biochar [7,12–14,21–24]. Acid-based activation is often preferred in certain applications because acidic agents are effective in removing surface impurities and modifying pore structure and surface chemistry. An activating agent widely used to produce engineered biochar for environmental applications is H_3PO_4 that has a lower corrosiveness than other acidic chemical activators [22].

This paper aimed at recovering vine pruning residues by slow pyrolysis and testing the engineered biochar obtained in the process as an adsorbent of VOC species. The experimental study consisted of 3 stages: (i) chemical pretreatment of vine residues with H_3PO_4 solutions; (ii) production of biochar (BC) and chemically activated biochar (ABC) by slow pyrolysis of non-impregnated and impregnated vine residues, respectively, in a fixed bed column, in the presence of CO_2 ; (iii) adsorption of 1,2-dichloroethane (DCE) from air stream onto BC and ABC in a fixed bed column. Quadratic polynomial models were used to predict the performances of pyrolysis and adsorption processes and determine the optimum levels of process factors.

2. Materials and methods

Plant material

Plant material consisted in vine pruning residues supplied by USAMV Bucharest [15,17,25].

Pretreatment of plant material

Vine pruning residues were pretreated according to the scheme of main operations shown in Fig. 1. The residues were cut with scissors resulting in cylindrical particles with mean dimensions (diameter \times length) of 0.35 cm \times 2.0 cm. About 90% of the amount of shredded residues was then impregnated with H_3PO_4 solutions of different concentrations, *i.e.*, 10%, 31%, 48%, and 52%, corresponding to impregnation ratios (IR) of 0.3 g/g, 1.1 g/g, 1.9 g/g, and 2.2 g/g, where IR is defined by Eq. (1) as mass of H_3PO_4 (m_{acid}) divided by mass of vine residues (m_{res}). The impregnations were performed in perfect mixing reactors (Fig. 2) for 2 h, then the suspensions were filtered and the impregnated material was dried in an oven for 12 h.

$$IR = \frac{m_{acid}}{m_{res}} \quad (1)$$

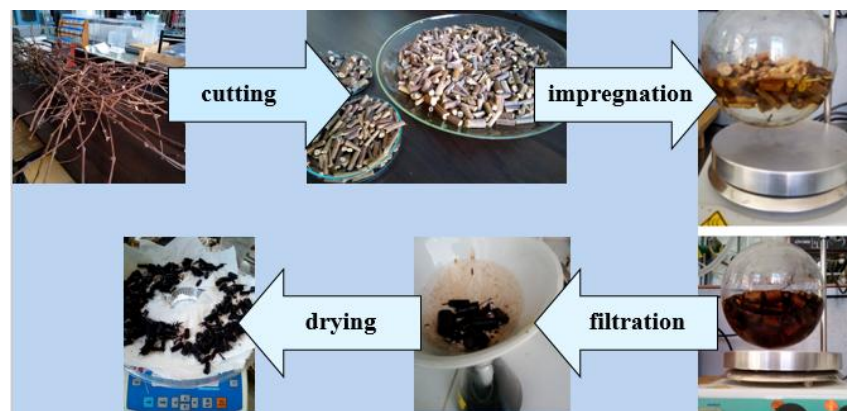


Fig. 1. Scheme of main operations for the pretreatment of vine pruning residues.



Fig. 2. Perfect mixing reactors used for impregnating shredded vine residues with H_3PO_4 solutions.

Production of BC and ABC by slow pyrolysis of non-impregnated and impregnated plant material

BC and ABC were produced by slow pyrolysis of non-impregnated and impregnated vine residues, using CO_2 as a sweeping gas and reactant in the process. The experimental setup and working procedure were detailed in a previous paper

[25]. A part of the pyrolysis setup is shown in Fig. 3. The shredded plant material was placed in the column (1), 3 cm internal diameter (D) and 50 cm height, set into the support (2). The column wall was heated by the electrical resistance (3) and thermally insulated by the glass cylinder (4). CO_2 was introduced into the column (1), upflowed through the fixed bed of plant material, and exited the column along with the vapour (V) and non-condensable gases (NCGs) obtained during the pyrolysis. The mixture of V and NCGs was cooled resulting in a liquid phase (bio-oil), which was collected in a graduated cylinder, and pyrolysis gases.

Mass of solid phase (m), mass of liquid phase (m_L), temperature in the center of biomass bed (t_c), and temperature at the column wall (t_w) were continuously measured. Mean logarithmic temperature of biomass bed (t_m) was calculated using Eq. (2).

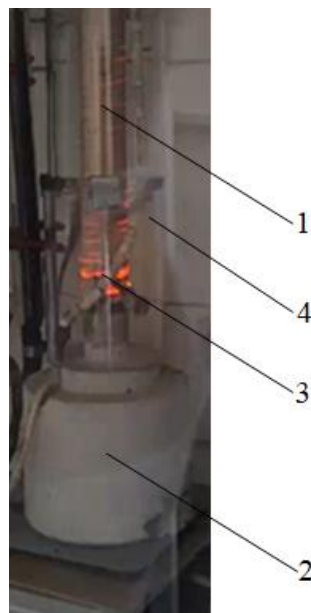


Fig. 3. Detail from the pyrolysis setup: (1) ceramic column; (2) support; (3) electrical resistance; (4) glass cylinder.

$$t_m = \frac{t_w - t_c}{\ln\left(\frac{t_w}{t_c}\right)} \quad (2)$$

According to a central composite design (CCD) with 2 independent variables (factors), 12 experiments (exp. 1–12 in Table 1) were performed for 60 min, at 1 atm, and at a level of CO_2 volumetric flow rate (G_V) of 10 L/h = 2.78 cm^3/s , corresponding to a superficial velocity (w) defined by Eq. (3) of 0.4 cm/s. Thermal flux ($q = 4.3\text{--}6.6 \text{ kW/m}^2$) and impregnation ratio ($IR = 0.0\text{--}2.2 \text{ g/g}$) were

chosen as process factors. Levels of dimensionless process factors (x_1 and x_2) defined by Eqs. (4) and (5) are also specified in Table 1. Final (f) values (at $\tau_f = 60$ min) of specific mass of solid phase (BC/ABC), m_f/m_0 , where m_0 (g) represents the initial mass of non-impregnated/impregnated vine residues, specific mass of liquid phase (bio-oil), m_{Lf}/m_0 , and mean logarithmic temperature of biomass bed, t_{mf} , were selected as dependent variables (responses) of pyrolysis process.

$$w = \frac{4G_V}{\pi D^2} \quad (3)$$

$$x_1 = \frac{q - 5.4}{0.8} \quad (4)$$

$$x_2 = \frac{IR - 1.1}{0.8} \quad (5)$$

Table 1
Experimental values of pyrolysis and adsorption responses at different levels of dimensional and dimensionless factors

Exp.	q (kW/m ²)	IR (g/g)	x_1	x_2	m_f/m_0 (g/g)	m_{Lf}/m_0 (g/g)	t_{mf} (°C)	$C_{if,ads}$ (g/g)
1	4.6	0.3	-1	-1	0.410	0.250	352	0.077
2	4.6	1.9	-1	1	0.522	0.230	360	0.112
3	6.2	0.3	1	-1	0.354	0.300	404	0.103
4	6.2	1.9	1	1	0.430	0.280	417	0.134
5	5.4	1.1	0	0	0.530	0.260	382	0.110
6	5.4	1.1	0	0	0.542	0.265	383	0.102
7	4.3	1.1	-1.414	0	0.481	0.237	345	0.093
8	6.6	1.1	1.414	0	0.377	0.334	422	0.136
9	5.4	0.0	0	-1.414	0.310	0.308	416	0.064
10	5.4	2.2	0	1.414	0.495	0.260	370	0.110
11	5.4	1.1	0	0	0.528	0.261	380	0.102
12	5.4	1.1	0	0	0.537	0.272	381	0.108
Minimum value (MIN)					0.310	0.230	345	0.064
Maximum value (MAX)					0.542	0.334	422	0.136
Mean value					0.460	0.271	384	0.104
Standad deviation (SD)					0.081	0.030	25.8	0.020

Testing BC and ABC as adsorbents of VOC from air stream

BC and ABC obtained by slow pyrolysis of non-impregnated and impregnated vine residues (exp. 1–12 in Table 1) were tested as adsorbents of DCE from air stream. DCE is a VOC with a boiling point of 83.5 °C at atmospheric pressure and a vapour pressure of 7.7 kPa at 20 °C.

The experimental setup and adsorption procedure were detailed in previous papers [26–28]. A part of the adsorption setup is shown in Fig. 4. BC/ABC was packed into the glass column (1), 1.7 cm internal diameter and 29 cm height, which was placed in the holder (2) and put on the digital balance (3) in an enclosure with

insulating polystyrene walls (4). Air was fed by a compressor into the silica gel column (5) to remove the humidity and further bubbled into the liquid VOC species from a bubbler. The mixture of air and VOC vapour exiting the bubbler was introduced into the adsorption column (1) and passed upward through the BC/ABC fixed bed until it was saturated. The finned heater (6) increased the temperature inside the insulating enclosure and maintained it at a constant value. The thermal agent in the heater (6) was warm water from the thermostatic bath (7). The amount of adsorbed VOC was estimated based on the increase in the mass of the adsorption column, considering that the saturation state was attained when the column mass did not vary for 10 min.

Twelve adsorption experimental runs were performed for 90 min at 40 °C, 1 atm, and a level of air superficial velocity of 0.7 cm/s. Final (f) values (at $\tau_{f,ads} = 90$ min) of BC/ABC adsorption capacity for *i* species of VOC ($C_{if,ads}$) defined by Eq. (6), where $m_{if,ads}$ (g) represents the mass of *i* species (DCE) adsorbed at $\tau_{f,ads}$ and $m_{BC/ABC,0}$ (g) the initial mass of BC/ABC, was selected as response of adsorption process.

$$C_{if,ads} = \frac{m_{if,ads}}{m_{BC/ABC,0}} \quad (6)$$



Fig. 4. Adsorption setup: (1) glass adsorption column; (2) holder; (3) digital balance; (4) insulating enclosure; (5) silica gel column; (6) finned heater; (7) water bath.

Statistical analysis

Statistical analysis was performed using STATISTICA version 10.0 (StatSoft Inc., Tulsa, OK, USA).

3. Results and discussion

Experimental values of pyrolysis and adsorption process responses ($m_f/m_0 = 0.310\text{--}0.542\text{ g/g}$, $m_{Lf}/m_0 = 0.230\text{--}0.334\text{ g/g}$, $t_{mf} = 345\text{--}422\text{ }^\circ\text{C}$, and $C_{if,ads} = 0.064\text{--}0.136\text{ g/g}$) at different levels of factors ($q = 4.3\text{--}6.6\text{ kW/m}^2$ and $IR = 0.0\text{--}2.2\text{ g/g}$) are summarized in Table 1. Relevant statistics of selected responses (*MIN*, *MAX*, mean value, and *SD*) are also specified in Table 1. It is observed that maximum values of m_{Lf}/m_0 , t_{mf} , and $C_{if,ads}$ were obtained in exp. 8 ($q = 6.6\text{ kW/m}^2$ and $IR = 1.1\text{ g/g}$, corresponding to $x_1 = 1.414$ and $x_2 = 0$), whereas minimum values of m_L/m_0 and $C_{if,ads}$ were obtained in exp. 9 ($q = 5.4\text{ kW/m}^2$ and $IR = 0$, corresponding to $x_1 = 0$ and $x_2 = -1.414$). Correlation analysis indicated a very strong positive correlation between m_{Lf}/m_0 and t_{mf} responses ($r = 0.9$) as well as strong negative correlations between m_f/m_0 and m_{Lf}/m_0 ($r = -0.7$) and m_f/m_0 and t_{mf} ($r = -0.6$), consistent with previous results [25,29–32].

The values of $C_{if,ads}$ were consisted with those reported in the literature. Khan et al. [18] used different types of biowaste-derived biochar to remove benzene from air and found values of $C_{if,ads}$ at 298 K of 0.35–144 mg/g. Papurello et al. [19] reported data on the adsorption of different trace compounds from the biogas obtained by anaerobic digestion of organic residues using wood waste-based biochar as an adsorbent. The values of $C_{if,ads}$ were higher for 2-butanone (158.8 mg/g), toluene (140.1 mg/g), and limonene (64 mg/g) than those for H₂S (1.05 mg/g) and hexamethylcyclotrisiloxane (1.28 mg/g). Zhang et al. [20] studied the adsorption of 3 VOC species (acetone, cyclohexane, and toluene) from gas streams onto 5 types of biochar (from bamboo, sugarcane bagasse, Brazilian pepper wood, sugar beet tailings, and hickory wood) obtained by slow pyrolysis performed at 3 levels of operating temperature (300 °C, 450 °C, and 600 °C). The values of $C_{if,ads}$ for all types of biochar were in the range 5.58–91.2 mg/g.

The effects of x_1 , x_1^2 , x_2 , x_2^2 , and x_1x_2 on y_j ($j = 1\text{--}4$) were quantified using quadratic (second-order) polynomial models given by Eq. (7), where $y_1 = (m_f/m_0)_{calc}$, $y_2 = (m_{Lf}/m_0)_{calc}$, $y_3 = t_{mf,calc}$, and $y_4 = C_{if,ads,calc}$ represent predicted (calculated) responses and β_{kj} ($k = 1\text{--}6$, $j = 1\text{--}4$) are regression coefficients.

$$y_j = \beta_{1j} + \beta_{2j}x_1 + \beta_{3j}x_1^2 + \beta_{4j}x_2 + \beta_{5j}x_2^2 + \beta_{6j}x_1x_2, j = 1\text{--}4 \quad (7)$$

Regression coefficients, which were determined based on experimental data specified in Table 1, are presented in Table 2 along with their *p*-values (p_{kj}), R^2 , R^2_{adj} , *RSE*, *F*, and *p*. The results summarized in Table 2 indicate the following relevant aspects: (i) a significant positive effect of x_2 (dimensionless impregnation ratio) and significant negative effects of x_1 (dimensionless thermal flux), x_1^2 , and x_2^2 on y_1 (specific mass of BC/ABC at $\tau_f = 60\text{ min}$); (ii) a significant positive effect of x_1 and a significant negative effect of x_2 on y_2 (specific mass of bio-oil at $\tau_f = 60\text{ min}$); (iii) a significant positive effect of x_1 on y_3 (mean logarithmic temperature of

BC/ABC bed at $\tau_f = 60$ min); (iv) a significant negative effect of x_2^2 and significant positive effects of x_1 , x_1^2 , and x_2 on y_4 (BC/ABC adsorption capacity for i species of VOC at $\tau_{f,ads} = 90$ min); (v) a good agreement between experimental and predicted data ($R^2 \geq 0.866$, $R^2_{adj} \geq 0.754$, $RSE \leq 12.79$, $F \geq 7.735$, $p \leq 0.014$).

Table 2
 Regression coefficients (β_{kj} , $k = 1 \dots 6$, $j = 1 \dots 4$) in Eq. (6) and related p -values (p_{kj}), multiple determination coefficient (R^2), adjusted R^2 (R^2_{adj}), residual standard error (RSE), F statistic (F), and p -value for F (p).

j		1		2		3		4	
Response		$y_1 = (m_f/m_0)_{calc}$		$y_2 = (m_{L_f}/m_0)_{calc}$		$y_3 = t_{mf, calc}$		$y_4 = C_{if, ads, calc}$	
Regressor	k	β_{k1}	p_{k1}	β_{k2}	p_{k2}	β_{k3}	p_{k3}	β_{k4}	p_{k4}
Intercept	1	0.534	0.0000	0.265	0.0000	381.5	0.0000	0.105	0.0000
x_1	2	-0.037	0.0003	0.030	0.0009	27.24	0.0009	0.014	0.0002
x_1^2	3	-0.049	0.0001	0.006	0.3468	-0.251	0.9620	0.006	0.0202
x_2	4	0.056	0.0000	-0.013	0.0325	-5.506	0.2689	0.016	0.0001
x_2^2	5	-0.063	0.0000	0.005	0.4112	4.500	0.4076	-0.008	0.0062
$x_1 x_2$	6	-0.009	0.2423	0.000	1.0000	1.250	0.8514	-0.001	0.6909
R^2		0.984		0.885		0.866		0.970	
R^2_{adj}		0.970		0.789		0.754		0.944	
RSE		0.014		0.014		12.79		0.005	
F		73.24		9.241		7.735		38.29	
p		0.000		0.009		0.014		0.000	

Statistically significant coefficients ($p_{kj} \leq \alpha = 0.05$, where α is the significance level) are written in bold.

Predicted values of pyrolysis and adsorption responses (y_j , $j = 1 \dots 4$) at different levels of dimensionless factors (x_1 and x_2), obtained using Eq. (7) with regression coefficients (β_{kj} , $k = 1 \dots 6$, $j = 1 \dots 4$) specified in Table 2, are summarized in Table 3 and shown in Figures 5–8. Table 3 also contains relevant indicators of position and variability of process responses. According to the data summarized in Tables 2 and 3, the results shown in Figures 5–8 emphasize the following: (i) y_1 increases with an increase in x_1 from -1.414 to about -0.7 (corresponding to $q = 4.8$ kW/m²) and decreases with an increase in x_1 from 0 to 1.414; y_1 increases with an increase in x_2 from -1.414 to 0 and decreases with an increase in x_2 from about 0.7 (corresponding to $IR = 1.7$ g/g) to 1.414; (ii) y_2 increases with an increase in x_1 and decreases with an increase in x_2 , the effect of x_1 being more pronounced; (iii) y_3 increases with an increase in x_1 , whereas the effect of x_2 on y_3 is negligible; (iv) y_4 is almost constant for x_1 in the range 1.414–0 and increases with an increase in x_1 from 0 to 1.414; y_4 increases with an increase in x_2 from -1.414 to 0 and is almost constant for x_2 in the range 0–1.414. Accordingly, based on the results presented in Table 3 and Figure 8, optimum levels of process factors, for which maximum predicted values of adsorption capacity ($y_4 = 0.137$ g/g) were attained, were $x_1 = 1.414$ and $x_2 = 0$, corresponding to $q = 6.6$ kW/m² and $IR = 1.1$ g/g (exp. 8 in Tables

1 and 3). Moreover, maximum predicted values of specific mass of bio-oil ($y_2 = 0.318 \text{ g/g}$) and mean temperature of BC/ABC bed ($y_3 = 420 \text{ }^\circ\text{C}$) were obtained at these optimum levels of process factors (Table 3).

Table 3
Predicted values of pyrolysis and adsorption responses at different levels of dimensionless factors

Exp.	x_1	x_2	y_1 (g/g)	y_2 (g/g)	y_3 ($^\circ\text{C}$)	y_4 (g/g)
1	-1	-1	0.394	0.259	365	0.073
2	-1	1	0.524	0.232	352	0.107
3	1	-1	0.338	0.318	417	0.102
4	1	1	0.433	0.291	409	0.133
5	0	0	0.534	0.265	382	0.105
6	0	0	0.534	0.265	382	0.105
7	-1.414	0	0.488	0.234	342	0.098
8	1.414	0	0.383	0.318	420	0.137
9	0	-1.414	0.330	0.293	398	0.067
10	0	1.414	0.489	0.255	383	0.113
11	0	0	0.534	0.265	382	0.105
12	0	0	0.534	0.265	382	0.105
Minimum value (MIN)		0.330	0.232	342	0.067	
Maximum value (MAX)		0.534	0.318	420	0.137	
Mean value		0.460	0.271	384	0.104	
Standad deviation (SD)		0.080	0.028	24.0	0.020	

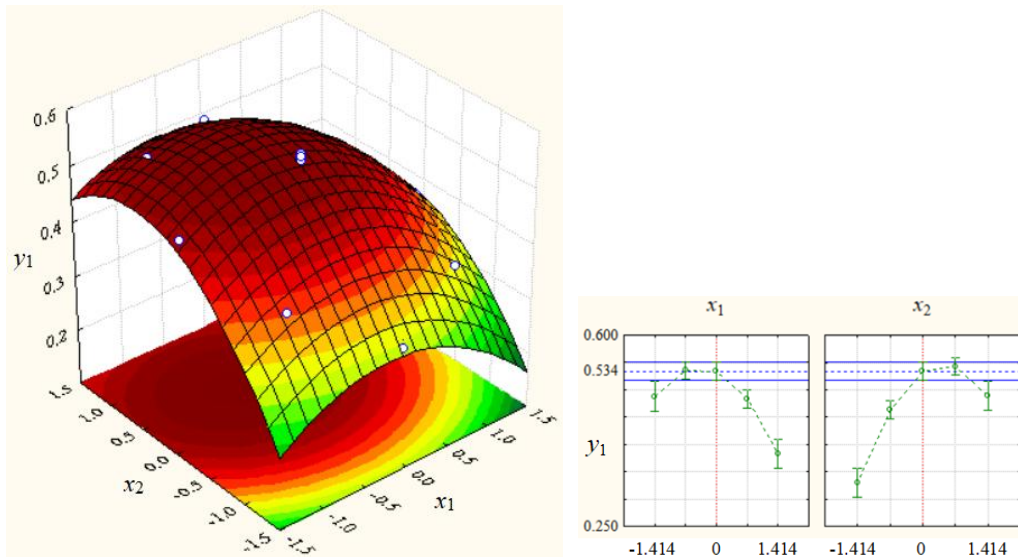
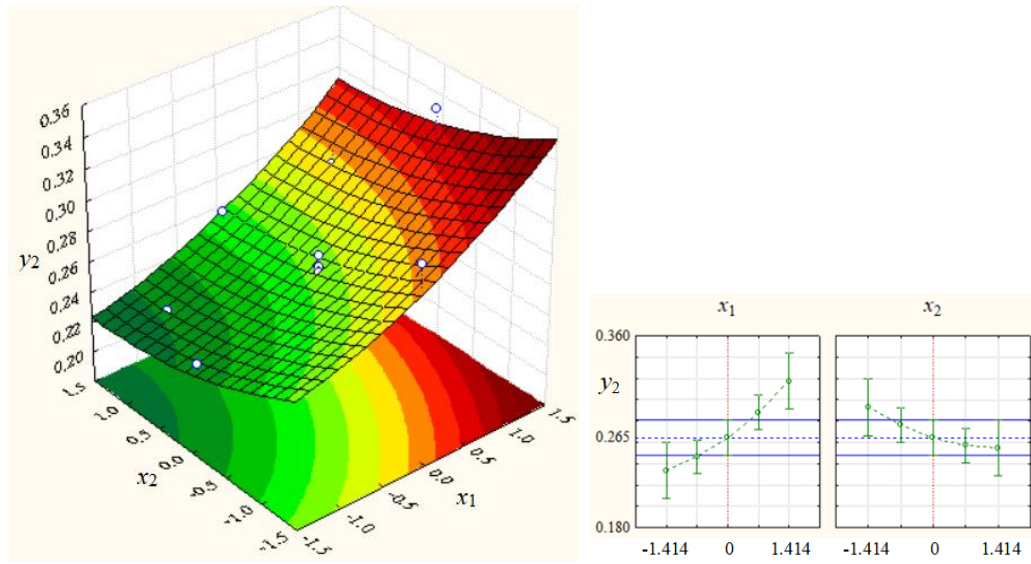
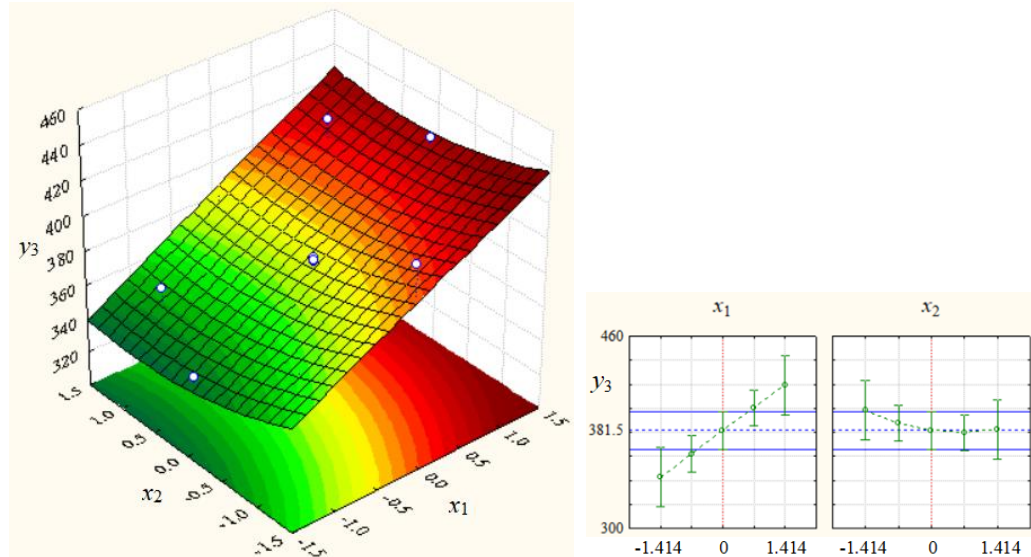


Fig. 5. Effects of dimensionless factors on $y_1 = (m_1/m_0)_{\text{calc.}}$

Fig. 6. Effects of dimensionless factors on $y_2 = (m_{Lf}/m_0)_{calc}$.Fig. 7. Effects of dimensionless factors on $y_3 = t_{mf,calc}$.

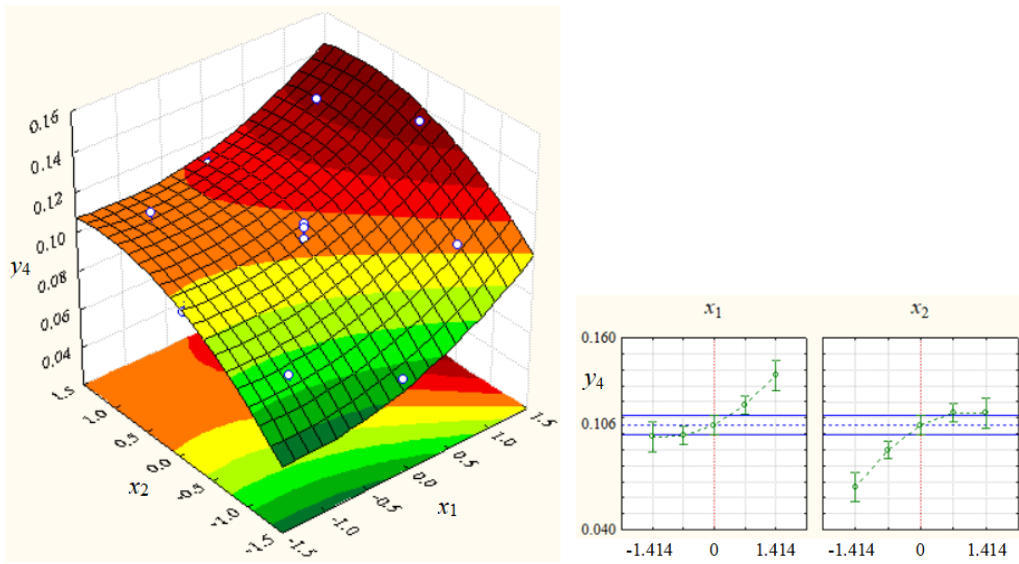


Fig. 8. Effects of dimensionless factors on $y_4 = C_{if,ads,calc}$.

4. Conclusions

The production of biochar (BC) and chemically modified biochar (ABC) from vine pruning residues, which are often burned, and application of BC/ABC as VOC adsorbents can have significant environmental and economic benefits.

Pyrolysis factors in terms of heat flux ($q = 4.3\text{--}6.6 \text{ kW/m}^2$) and impregnation ratio ($IR = 0\text{--}2.2 \text{ g/g}$) affected pyrolysis and adsorption performances as follows: (i) specific mass of BC/ABC ($m_f/m_0 = 0.310\text{--}0.542$) decreased significantly as q increased from 5.4 kW/m^2 to 6.6 kW/m^2 and IR decreased from 1.1 g/g to 0 (no impregnation); (ii) q had a significant positive effect on specific mass of bio-oil ($m_{L_f}/m_0 = 0.230\text{--}0.334 \text{ g/g}$) and mean temperature of BC/ABC bed ($t_{mf} = 345\text{--}422 \text{ }^\circ\text{C}$); (iii) BC/ABC adsorption capacity for DCE ($C_{if,ads} = 0.064\text{--}0.136 \text{ g/g}$) increased with an increase in q and IR , the increase being significant for $q = 5.4\text{--}6.6 \text{ kW/m}^2$ and $IR = 0\text{--}1.1 \text{ g/g}$. Moreover, m_{L_f}/m_0 and t_{mf} were very strongly positively correlated, whereas m_f/m_0 and m_{L_f}/m_0 as well as m_f/m_0 and t_m were strongly negatively correlated.

The effects of q and IR on selected responses were quantified using second-order polynomial models. Maximum predicted values of adsorption capacity (0.137 g/g), specific mass of bio-oil (0.318 g/g) and mean temperature of BC/ABC bed ($420 \text{ }^\circ\text{C}$) were obtained at $q = 6.6 \text{ kW/m}^2$ and $IR = 1.1 \text{ g/g}$.

Acknowledgments

This work was supported by a grant of the Romanian Ministry of Education and Research, CCCDI—UEFISCDI, project number 372PED/2020 (PN-III-P2-2.1-

PED-2019-4917), within PNCDI III.

R E F E R E N C E S

- [1] *F. Amalina, A.S. Abd Razak, S. Krishnan, H. Sulaiman, A.W. Zularisam, M. Nasrullah*, Biochar production techniques utilizing biomass waste-derived materials and environmental applications – A review, *J. Hazard. Mater.*, **vol. 7**, 2022, 100134.
- [2] *O. Awogbemi, D.V. Von Kallon*, Progress in agricultural waste derived biochar as adsorbents for wastewater treatment, *Appl. Surf. Sci. Adv.*, **vol. 18**, 2023, 100518.
- [3] *P. Premchand, F. Demichelis, D. Chiaramonti, S. Bensaid, D. Fino*, Study on the effects of carbon dioxide atmosphere on the production of biochar derived from slow pyrolysis of organic agro-urban waste, *Waste Manag.*, **vol. 172**, 2023, pp. 308–319.
- [4] *W. Gwenzi, N. Chaukura, T. Wenga, M. Mtisi*, Biochars as media for air pollution control systems: Contaminant removal, applications and future research directions, *Sci. Total Environ.*, **vol. 753**, 2021, 142249.
- [5] *O.C.N. Ndoung, C.C. de Figueiredo, M.L.G. Ramos*, A scoping review on biochar-based fertilizers: Enrichment techniques and agro-environmental applications, *Helion*, **vol. 7**, 2021, e08473.
- [6] *I. Vassura, D. Fabbri, A.G. Rombolà, B. Rizzi, A. Menichetti, S. Cornali, L. Pagano, R. Reggiani, M.R. Vecchi, N. Marmiroli*, Multi-analytical techniques to study changes in carbon and nitrogen forms in a tomato-cultivated soil treated with biochar and biostimulants, *Soil & Environmental Health*, **vol. 1**, no. 4, 2023, 100050.
- [7] *Z. Zhao, B. Wang, B.K.G. Theng, X. Lee, X. Zhang, M. Chen, P. Xu*, Removal performance, mechanisms, and influencing factors of biochar for air pollutants: A critical review, *Biochar*, **vol. 4**, no. 1, 2022, 30.
- [8] *M. Balat, M. Balat, E. Kirtay, H. Balat*, Main routes for the thermo-conversion of biomass into fuels and chemicals. Part 1: Pyrolysis systems, *Energ. Convers. Manage.*, **vol. 50**, 2009, pp. 3147–3157.
- [9] *S.S. Senadheera, S. Gupta, H.W. Kua, D. Hou, S. Kim, D.C.W. Tsang, Y.S. Ok*, Application of biochar in concrete – A review, *Cem. Concr. Compos.*, **vol. 143**, 2023, 105204.
- [10] *K.S.D. Premarathna, A.U. Rajapaksha, B. Sarkar, E.E. Kwon, A. Bhatnagar, Y.S. Ok, M. Vithanage*, Biochar-based engineered composites for sorptive decontamination of water: A review, *Chem. Eng. J.*, **vol. 372**, 2019, pp. 536–550.
- [11] *A.U. Rajapaksha, S.S. Chen, D.C.W. Tsang, M. Zhang, M. Vithanage, S. Mandal, B. Gao, N.S. Bolan, Y.S. Ok*, Engineered/designer biochar for contaminant removal/immobilization from soil and water: Potential and implication of biochar modification, *Chemosphere*, **vol. 148**, 2016, pp. 276–291.
- [12] *B. Wang, B. Gao, J. Fang*, Recent advances in engineered biochar productions and applications. *Crit. Rev. Environ. Sci. Technol.*, **vol. 47**, no. 22, 2017, pp. 2158–2207.
- [13] *J. Wang, S. Wang*, Preparation, modification and environmental application of biochar: A review, *J. Clean. Prod.*, **vol. 227**, 2019, pp. 1002–1022.
- [14] *C. Zhang, S. Sun, S. Xu, C. Wu*, CO₂ capture over steam and KOH activated biochar: Effect of relative humidity, *Biomass Bioenergy*, **vol. 166**, 2022, 106608.
- [15] *S.I. Calcan, O.C. Pârvulescu, V.A. Ion, C.E. Răducanu, L. Bădulescu, R. Madjar, T. Dobre, D. Egri, M. Andrei, L.M. Iliescu, et al.*, Effects of biochar on soil properties and tomato growth, *Agronomy*, **vol. 12**, no. 8, 2022, 1824.
- [16] *L. Ceatru, O.C. Pârvulescu, I. Rodriguez Ramos, T. Dobre*, Preparation, characterization, and testing of a carbon-supported catalyst obtained by slow pyrolysis of nickel salt impregnated vegetal material, *Ind. Eng. Chem. Res.*, **vol. 55**, no. 6, 2016, pp. 1491–1502.

[17] *D. Egri, O.C. Pârvulescu, V.A. Ion, C.E. Răducanu, S.I Calcan, L. Bădulescu, R. Madjar, C. Orbeci, T. Dobre, A. Moț, et al.*, Vine pruning-derived biochar for agronomic benefits, *Agronomy*, **vol. 12**, no. 11, 2022, 2730.

[18] *A. Khan, J.E. Szulejko, P. Samaddar, K.H. Kim, B. Liu, H.A. Maitlo, X. Yang, Y.S. Ok*, The potential of biochar as sorptive media for removal of hazardous benzene in air, *Chem. Eng. J.*, **vol. 361**, 2019, pp. 1576–1585.

[19] *D. Papurello, A. Boschetti, S. Silvestri, I. Khomenko, F. Biasioli*, Real-time monitoring of removal of trace compounds with PTR-MS: Biochar experimental investigation, *Renew. Energy*, **vol. 125**, 2018, pp. 344–355.

[20] *X. Zhang, B. Gao, Y. Zheng, X. Hu, A.E. Creamer, M.D. Annable, Y. Li*, Biochar for volatile organic compound (VOC) removal: Sorption performance and governing mechanisms, *Bioresour. Technol.*, **vol. 245**, 2017, pp. 606–614.

[21] *C.H. Pimentel, L. Diaz-Fernández, D. Gómez-Díaz, M.S. Freire, J. González-Alvarez*, Separation of CO₂ using biochar and KOH and ZnCl₂ activated carbons derived from pine sawdust, *J. Environ. Chem. Eng.*, **vol. 11**, no. 6, 2023, 111378.

[22] *B. Sajjadi, T. Zubatiuk, D. Leszczynska, J. Leszczynski, W.Y. Chen*, Chemical activation of biochar for energy and environmental applications: A comprehensive review, *Rev. Chem. Eng.*, **vol. 35**, no. 7, 2018, pp. 777–815.

[23] *Z. Wang, Q. Wang, X. Yang, S. Xia, A. Zheng, K. Zeng, Z. Zhao, H. Li, S. Sobek, S. Werle*, Comparative assessment of pretreatment options for biomass pyrolysis: Linking biomass compositions to resulting pyrolysis behaviors, kinetics and product yields, *Energy Fuels*, **vol. 35**, no. 4, 2021, pp. 3186–3196.

[24] *C.Y. Xu, Q.R. Li, Z.C. Geng, F.N. Hu, S.W. Zhao*, Surface properties and suspension stability of low-temperature pyrolyzed biochar nanoparticles: Effects of solution chemistry and feedstock sources, *Chemosphere*, **vol. 259**, 2020, 127510.

[25] *S.I. Calcan, O.C. Pârvulescu, V.A. Ion, C.E. Răducanu, L. Bădulescu, T. Dobre, D. Egri, A. Moț, V. Popa, M.E. Crăciun*, Valorization of vine prunings by slow pyrolysis in a fixed-bed reactor, *Processes*, **vol. 10**, no. 1, 2022, 37.

[26] *T. Dobre, O.C. Pârvulescu, G. Iavorschi, M. Stroescu, A. Stoica*, Volatile organic compounds removal from gas streams by adsorption onto activated carbon, *Ind. Eng. Chem. Res.*, **vol. 53**, 2014, pp. 3622–3628.

[27] *T. Dobre, O.C. Pârvulescu, A. Jacquemet, V.A. Ion*, Adsorption and thermal desorption of volatile organic compounds in a fixed bed—experimental and modeling, *Chem. Eng. Commun.*, **vol. 203**, no. 12, 2016, pp. 1554–1561.

[28] *V.A. Ion, O.C. Pârvulescu, T. Dobre*, Volatile organic compounds adsorption onto neat and hybrid cellulose, *Appl. Surf. Sci.*, **vol. 335**, 2015, pp. 137–146.

[29] *D.R. Cioroiu, O.C. Pârvulescu, T. Dobre, C. Răducanu, C.I. Koncsag, A. Mocanu, N. Duțeanu*, Slow pyrolysis of *Cystoseira barbata* brown macroalgae, *Rev. Chim.*, **vol. 69**, no. 3, 2018, pp. 553–556.

[30] *T. Dobre, O.C. Pârvulescu, G. Iavorschi, A. Stoica, M. Stroescu*, Catalytic effects at pyrolysis of wheat grains impregnated with nickel salts, *International Journal of Chemical Reactor Engineering*, **vol. 8**, 2010, pp. 1968–1992.

[31] *T. Dobre, O.C. Pârvulescu, I. Rodriguez Ramos, L. Ceatră, M. Stroescu, A. Stoica, R. Mirea*, Global reaction kinetics and enthalpy in slow pyrolysis of vegetal materials, *Rev. Chim.*, **vol. 63**, no. 1, 2012, pp. 54–59.

[32] *O.C. Pârvulescu, T. Dobre, L. Ceatră, G. Iavorschi, R. Mirea*, Characteristics of corn grains pyrolysis in a fixed bed reactor, *Rev. Chim.*, **vol. 62**, no. 1, 2011, pp. 89–94.